CHEMIJA. 2013. Vol. 24. No. 4. P. 260–270

Electrooxidation of borohydride on a polycrystalline platinum electrode

Dijana Šimkūnaitė*,

Loreta Tamašauskaitė-Tamašiūnaitė,

Svetlana Lichušina

State Research Institute
Center for Physical Sciences and Technology,
A. Goštauto St. 9,
LT-01108 Vilnius,
Lithuania

Electrochemical impedance spectroscopy and cyclic voltammetry techniques were employed to study borohydride oxidation on a polycrystalline Pt electrode in an aqueous alkaline media containing 0.05 M $NaBH_4$ and 1 M NaOH. Determined current density changes were interpreted in combination with EIS measurements. The regions of decreasing anodic current leading to negative polarization resistance, R_p, were supposed to be appreciably related to increasing availability of oxygen-containing species (OH_{ad} and Pt oxides) on the Pt surface in the presence of the accumulated borohydride species. Possible borohydride oxidation processes and electrical circuits were discussed regarding the potential applied.

Key words: borohydride oxidation, platinum electrode, electrochemical impedance spectroscopy, cyclic voltammetry

INTRODUCTION

Direct borohydride fuel cells (DBFCs), employing sodium borohydride ($NaBH_4$) aqueous solution as fuel, are highly promising energy generators for mobile and portable electronic devices [1–3]. They are very attractive mainly due to their high energy density (9.3 Wh · g^{-1} for $NaBH_4$ and 6.5 Wh · g^{-1} KBH_4), high open circuit voltage (1.64 V) and borohydride oxidation reaction (BOR) with theoretically complete eight-electrons per borohydride ion. The processes proceeding on the electrodes in DBFCs are as follows:

Anode:

$$BH_4^- + 8OH^- \rightarrow BO_2^- + 6H_2O + 8e^- \quad (E^0 = -1.24 \text{ V vs SHE}); \quad (1)$$

Cathode:

$$2O_2 + 4H_2O + 8e^- \rightarrow 8OH^- \quad (E^0 = 0.4 \text{ V vs SHE}); \quad (2)$$

Overall reaction:

$$BH_4^- + 2O_2 \rightarrow BO_2^- + 2H_2O \quad (E_{cell} = 1.64 \text{ V vs SHE}). \quad (3)$$

Nevertheless, numerous investigations initiated as far back as 1990s, the mechanism of BOR has not been completely understood up to now. The net oxidation reaction is rather complex and complicated [4–11]. It markedly depends on catalyst material, solution composition ($[BH_4^-]$/$[OH^-]$ ratio) and potential applied. A variety of intermediates can be formed at the electrode surface due to the dissociative adsorption of BH_4^- on Pt, Ir, Ag, Pd [11–13] or molecular $BH_{4,ad}^-$ adsorption on Os, Rh, Ru, Au [13, 14]. Besides, the rate of overall BOR process, involving complete eight-electrons per BH_4^- ion, is governed by contribution of a number of parallel individual competing oxidation pathways with the lower number of exchanged electrons and / or by heterogeneous chemical hydrolysis. The former reaction, resulting in hydrogen evolution, can be represented by

* Corresponding author. E-mail: nemezius@ktl.mii.lt

$$BH_4^- + H_2O \rightarrow BH_3OH^- + H_2. \quad (4)$$

It is deemed that both intermediates are capable of subsequent oxidation [5–7, 16, 17]:

$$H_2 + 2OH^- \rightarrow 2H_2O + 2e^-, \quad (5)$$

$$BH_3OH^- + 3OH^- \rightarrow BO_2^- + 3/2\ H_2 + 2H_2O + 3e^-, \quad (6)$$

or

$$BH_3OH^- + 6OH^- \rightarrow BO_2^- + 5\ H_2 + 2H_2O + 6\ e^-. \quad (7)$$

The principal drawback in the performance of DBFCs is an unfavoured hydrolysis reaction with hydrogen evolution (4) that results in the decrease of faradaic efficiency and reduced power density. This reaction is known to be heterogeneously catalyzed on several metals and metal oxides or alloys [15–17]. Therefore extensive investigations for highly efficient anode catalysts being able to suppress hydrogen are essential in advancing the application of DBFCs. The topping electrocatalysts are gold and platinum or materials modified with nanoparticles of those metals. Au represents one group of catalysts that typically demonstrate catalytic inactivity towards borohydride hydrolysis reaction [8, 16–20]. However, this group of the catalysts performs rather sluggish kinetics. Moreover, recently [10, 21–24] Au was shown to be unable to electrooxidise the whole hydrogen formed completely and therefore cannot be considered as a faradaic-efficient BOR electrocatalyst.

Despite the promotion of the heterogeneous hydrolysis of borohydride, Pt, representing another group of catalysts, demonstrates rather fast BOR kinetics and remains one of the most efficient catalysts for its oxidation. In the vast majority of the catalysts studied no practical electrocatalysts distinguished for both fast BOR kinetics and high faradaic efficiency have been determined for now. However, the interpretation of the processes occurring in the wide potential region even on Pt electrodes differs significantly, regardless the multiplicity hypothesis and proposed pathways of BH_4^- electrooxidation coincide well for experimental evidence [9, 11, 19, 25–27]. Recent studies of borohydride oxidation have been carried at various pH and different borohydride concentration by different techniques, involving cyclic voltammetry (CV) on stationary or rotating disk electrodes [6, 9, 19], electrochemical quartz crystal microbalance (EQCM) [26], in situ Fast Transform Infrared Spectroscopy (FTIR) and Differential Electrochemical Mass Spectrometry (DEMS) [10, 11, 22]. However, almost no studies on Pt catalyst were performed by the electrochemical impedance spectroscopy (EIS) method, which has been regarded as an effective and practical one for probing the interfacial features of the electrode surface. The only, more detailed and thorough analysis of borohydride oxidation with rather complex equations derived for impedance were performed on Au and are presented [28, 29]. Variations in fundamental characteristics ranging from phase transition to electrical conductivity can be induced by controlling the size and shape of the particles. In order to obtain the desirable quality of electrocatalysts composition the closer examination of BOR mechanism and kinetics on metals catalysts by combining several techniques is of much importance. Therefore, in the present work we reasoned to make preliminary investigations of borohydride oxidation on the polycrystalline Pt electrode in wide potential range by combining cyclic voltammetry and electrochemical impedance spectroscopy techniques.

EXPERIMENTAL

Electrochemical measurements were carried out in a conventional three-electrode cell containing 1M NaOH (Chempur Company) and 0.05 M $NaBH_4$ (Sigma-Aldrich Supply) at 20 ± 1 °C. Analytical grade chemicals and triply distilled water were used to prepare the solutions. Prior to each experiment, the working solution was deaerated with Ar for 0.5 h. The working electrode was a vertical disc of 1 cm^2, made from a polycrystalline Pt foil (99.99% purity, Russia). The counter electrode was a Pt sheet of ca. 4 cm^2 in area. Electrode potentials (E) were measured in reference to the Ag|AgCl|KCl(sat) electrode, unless otherwise stated.

The pretreatment of the electrode prior to each electrochemical measurement was as follows: (i) mechanical polishing to a nearly mirror finish with successively finer grades of alumina powders, eventually to 0.05 μm, and it was cleaned ultrasonically in sequence in acetone, diluted in HCl and triply distilled water; (ii) in order to obtain a clean reproducible surface before each following measurement, the Pt electrode was also scanned in the background of 0.5 M H_2SO_4 solution at a potential scan rate (v) 0.01 V · s^{-1} for 30 min between $E \approx -0.15$ and $E \approx +1.1$ V.

Cyclic voltammograms and impedance spectra were recorded using an μAutolab Type III. EIS measurements were carried out under potentiostatic conditions within the frequency (f) range from 1 Hz to 8 kHz with the perturbation amplitude of 5 mV. Some impedance spectra were analyzed invoking appropriate equivalent circuits.

RESULTS AND DISCUSSION

Figure 1a shows the cyclic voltammogram recorded for the polycrystalline Pt electrode in an alkaline 1 M NaOH solution at the scan rate 0.01 V s^{-1}. It can be characterized by the following three potential regions: (a) hydrogen adsorption / desorption region (–0.9 < E < –0.6 V), (b) double layer region (–0.6 < E < –0.45 V), and (c) hydroxide-oxide formation region (–0.45 < E < 0.6 V). Regarding the potential region applied two kinds of oxygen containing species PtOH and PtO can be generated by the mechanism proposed in [30]. Nevertheless, rather poor literature is available in alkaline solutions for the polycrystalline Pt electrode, how-

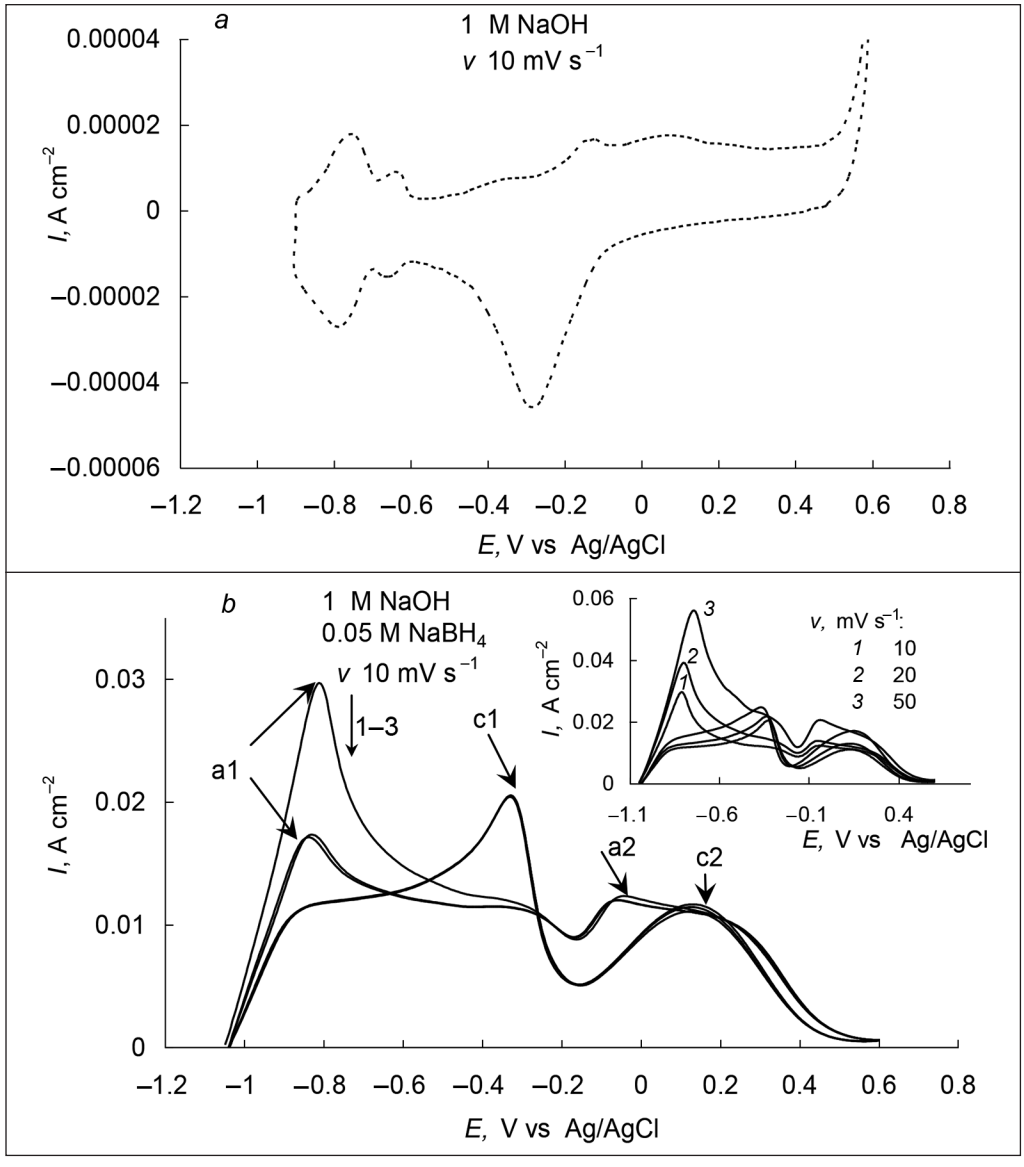

Fig. 1. Cyclic voltammograms obtained for the Pt electrode in the 1 M NaOH solution (*a*) and in the 1 M NaOH + 0.05 M $NaBH_4$ (*b*) at the scan rate $v = 10$ mV s^{-1}. The inset shows cyclic voltammograms obtained for the Pt electrode in the 1 M NaOH + 0.05 M $NaBH_4$ at different anodic *v*

ever, potential region up to ca. –0.10 V is commonly related to OH^- ions electrosorption with charge transfer and formation of surface hydroxides [31–33]:

$$OH^- \rightarrow OH_{ad} + e^-. \quad (8)$$

The former potential domain is associated with the reversible and weak OH_{ad} adsorption process before the oxide layer formation. Provided that OH_{ad} competes for the surface sites with H_2O molecules, electrosorption reaction (8) occurs to be not a simple OH^- ion discharge but rather a displacement reaction of the type [31]:

$$M–(H_2O)_x + OH^- \leftrightarrow M–OH + xH_2O + e^-. \quad (9)$$

More positive *E* domain is related to the formation of more irreversible and strong bounded OH_{ad} species and higher valent oxides on Pt(111) [30, 32, 33]. For polycrystalline Pt similar oxidation regions were observed [34, 26] and are close to our recorded ones. The most positive potential region ranging up to 0.6 V is attributed to stoichiometrically different Pt-OH species, that transform into $Pt\text{-}O^-$, Pt = O or Pt_2 = O highly depending on the surface coverage of strongly adsorbed OH_{ad} [26].

However, the above mentioned processes in the alkaline medium are not well separated in potential ranges as it is in the case of the acidic medium [35, 36]. Coupled H and OH adsorption / desorption processes in alkaline media are thought to occur reversibly up to ca. 0.65 V vs RHE on Pt(100) and Pt(110). The onset of OH^- adsorption on Pt in the alkaline medium starts quite early at ca. 0.35 V vs RHE [35, 36] as soon as desorption of H ceases. It is necessary to point that the presence of small amounts of adsorbed OH_{ad} species on the Pt(hkl) surface even in the H_{upd} region

in alkaline solutions were proved [32, 37]. Thus, the coupled competing adsorption / desorption process of H_{upd} and OH_{ad} in the H_{upd} region influences borohydride oxidation processes on Pt in the alkaline medium. Therefore, to decrease the rate of hydrogen evolution, which is commonly involved in borohydride oxidation processes and is related to a drastic current increase at low potentials, we get use of the above mentioned features and performed our experiments applying higher hydroxyl anion concentration [38].

Cyclic voltammograms of 0.05 M $NaBH_4$ oxidation on the polycrystalline Pt electrode during consecutive CV scans in the 1 M NaOH solution at 0.01 V s^{-1} are presented in Fig. 1b. The pronounced anodic current peak at low potentials on the first scan is observed. It reduces appreciably with further cycling. Practically reproducible voltammograms appear in a few successive cycles. To avoid notable dissolution of glass and thus distortion of CV curves by dissolved impurities from glass in the concentrated alkaline solution [39, 40] further cycling was not continued any longer. Obtained voltammetric data at different scan rates (Fig. 1b inset), as well as these reported in [9, 19, 26], show that voltammograms do not undergo radical transformations with the potential scan rate and are similar in shape. CV curves are typically associated with four characteristic oxidation peaks, i. e. two on the positive-going sweep and another two on the negative-going sweep labeled as a1, a2, c1 and c2, respectively. They are defined by the waves broadly lying in potential regions between –1 and –0.3 V and between –0.15 and 0.6 V on the anodic scan, followed by another two waves between 0.6 and –0.15 V and between –0.2 and –1 V on the cathodic scan.

Voltammograms over the polycrystalline Pt electrode in 1 M NaOH in the absence and in the presence of 0.05 M $NaBH_4$ show that defined currents are much larger in the former case than those due to H_{upd} desorption and Pt oxidation (Fig. 1a, b). Borohydride oxidation over the polycrystalline Pt electrode starts before the hydrogen oxidation occurs since the BH_4^- open circuit potential is at more negative potential than H_2 on Pt and the BH_3OH^- oxidation potential is considered to be more negative than BH_4^- [19]. Therefore, at low potentials current is supposed to increase due to BH_4^- oxidation, resulting in peak a1. Here the process is complicated by hydrolysis reaction (4) and is followed by reactions (5–7) in the broadly lying potential domain of wave a1 up to –0.3 V. The above mentioned wide potential domain of CV curves coincides with the response for the positive-going potential scan in the supporting electrolyte where weak and reversible OH_{ad} electrosorption by reaction (9) occurs. The oxygen source for borohydride oxidation here is assumed to be OH^- ions from the solution by the Eley-Rideal-type mechanism [19, 26].

After peak a1, current sharply decreases, passes a dip at ca. –0.18 V and a new oxidation peak a2 appears in the potential region of the second anodic wave a2 between –0.15 and 0.6 V (Fig. 1b). It is supposed that in this potential domain borohydride oxidation mechanism changes and proceeds on the partially oxidised Pt surface with irreversibly adsorbed OH_{ad} or Pt oxides formed. Therefore BH_4^- oxidation in the potential domain of wave a2 is less efficient than on bare platinum and is commonly attributed to direct BH_4^- oxidation pathway with 5 or 6 e^- involved [9, 26]. The oxygen source for borohydride oxidation involves adsorbed OH_{ad} by the Langmuir-Hinshelwood-type mechanism [26]. More extensive Pt oxide formation at potentials above ca. 0.1 V points to the suppression of borohydride oxidation. The change in the oxide structure is supposed and a negative current / potential slope is visible in cyclic voltammograms.

However, up till now the studies do not agree neither on the peak nor wave assignments in CV curves for BH_4^- oxidation on Pt. Recent electrochemical studies suggest that electrooxidation of BH_4^- on Pt at low potentials proceeds via direct pathway [9, 25], indirect pathway [19, 26, 27], and by partial borohydride hydrolysis or direct BOR [11]. Similarly, at higher potentials the indirect pathway, by which BH_3OH^- and H_2 could be formed and consequently oxidised, was proposed [9] and not ruled out by FTIR spectroscopy [11].

On the reverse potential scan two new anodic peaks appear. One comes before Pt oxide is reduced, the other Pt oxide reduction passed. They are denoted as peaks c2 and c1, respectively, and are located in potential domains of waves c2 and c1 between 0.6 and –0.15 V and between –0.2 and –1 V, respectively. Both of them are considered to have a "cleaning" effect on the Pt electrode surface. However, their interpretation also faces some differences. Wave c2 is assumed to correspond to BH_4^- oxidation and is associated with removal of Pt surface hydroxides or oxides in the dip of CV curve at ca. –0.18 V, while peak c1 corresponds to oxidation of $BH_3OH^-_{ad}$'s surface-adsorbed oxidation product [9]. Peaks c1 and c2 were attributed to oxidation of intermediates, such as BH_2OH_{ad} and BOH_{ad}, respectively [26].

It is necessary to point out some features inherent to BH_4^- oxidation on Pt. A complicated mechanism of borohydride oxidation is known to be dissociative and suggests a lot of species that could take part in adsorption processes [11, 12]. Adsorption of BH_4^- on Pt can occur already under open circuit conditions leading to spontaneous hydrolysis by Eq. (4), involving an initial pre-dissociation step at the active surface sites considering abstraction of hydrides [41]. Initial dissociative adsorption of BH_4^- ions over the Pt surface is highly favourable at all potentials of interest (including open circuit potential) if sufficient free Pt sites are available [12].

The qualitative features of experimentally recorded typical EIS spectra over large potential window are shown in Fig. 2. To avoid instability and / or irreproducibility of the system at low potentials generated by H_2 formation, which could gradually cover the Pt electrode surface even at high pH in borohydride solutions, we restricted ourselves in the E range from –0.4 V to +0.25 V.

The EIS data indicate that borohydride oxidation on Pt at various potentials shows different impedance behaviours. They can be subdivided into two groups accordingly to the sign of the real component Z' in the Nyquist plots (Fig. 2). In

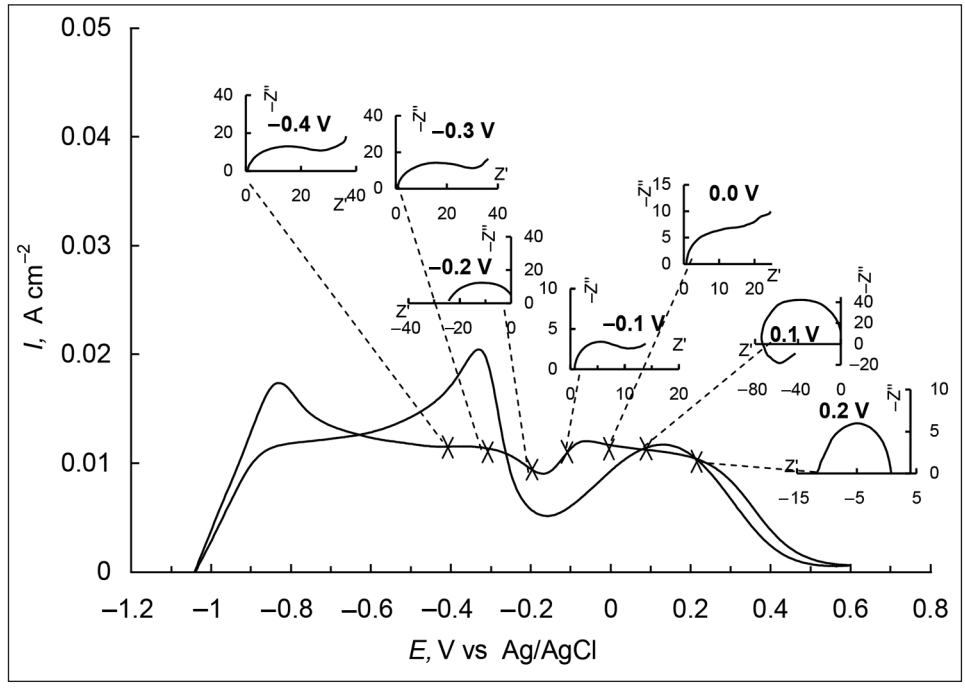

Fig. 2. Summary of the EIS behaviours shown by Nyquist diagram insets at selected potentials on the cyclic voltammogram

each group, Nyquist plots (interrelations between real, Z', and imaginary, Z'', components) are quite similar in shape though their quantitative characteristics can be rather different depending on the potential applied.

To describe the faradaic process of a catalytic reaction on the electrode surface an equivalent circuit model, consisting of a charge transfer resistance (R_{ct}) in parallel with a constant phase element (CPE) and a serial solution resistance component, is commonly used. R_{ct} is treated as an indicative of the rate of electrochemical reaction. In all cases it is a positive number and its value can be determined from an impedance arc at a low frequency. Often R_{ct} is related to the polarization resistance (R_p), which is denoted as the reciprocal of the slope of the steady state *I–E* curve and its value can be obtained from the impedance at the zero frequency limit [42]:

$$R_p = \lim_{w \to 0} Z(w) = \left(\frac{dj_{ss}}{dE} \right)^{-1}, \quad (10)$$

where j_{ss} is a steady state current limit. The values of R_{ct} and R_p are the same when the applied potential is the only state variable. However, in a complex heterogeneous kinetic system (e. g. anodic methanol oxidation and corrosion reactions), where surface coverage of the adsorbed species could be the additional state variable, complex impedance spectra spanning different axis quadrants like negative R_p could occur [43, 44]. Analogous negative R_p values are observed in our case for *E* regions ca. –0.2 V and from 0.1V to 0.25 V (Fig. 2). Therefore, to obtain an interrelation between impedance and voltammetric data, we made use of the relationship (10), according to which the polarization resistance can be treated as the limit of the faradaic impedance at low frequencies. Considering this relation in a qualitative sense, one can conclude that both the low-frequency Z' and the steady-state voltammetric slope should be of the same sign at the certain *E* (the so-called "hidden" negative impedance is supposed to be absent). The latter supposition is appreciably supported by experimental data shown in Fig. 2 since the voltammetric slopes are almost similar for the direct and reverse *E* scan over the entire region of potentials, where impedance measurements were performed and, besides, they coincide in sigh with low-frequency impedance data.

More detailed Nyquist and corresponding Bode plots of borohydride oxidation on the Pt electrode at different potentials applied are presented in Figs. 3–4. At *E* between –0.4 and –0.3 V the semi-circles are observed in the first quadrant. The diameters of the arcs increase slightly with the increase of potential indicating an increasing polarization resistance (Fig. 3a). In Bode plots only one broad peak for –0.4 and –0.3 V is defined (Fig. 4a) pointing to the only one reaction on the electrode. Evidently there is only the single "kinetically significant" adsorbed species, nevertheless, a variety of them can be discussed [9, 11, 12, 26]. At –0.2 V, a sudden change of the impedance pattern in the Nyquist plots happens with the arc transition from the first quadrant to the second one. The corresponding phase angle at low frequencies runs above 90°, indicating the presence of a negative polarization resistance R_p that usually results from passivation of the electrode surface. Similar negative impedance patterns were reported in the literature of corrosion process investigating the metal passivation during metal anodic dissolution [45, 46]. They were explained by the increasing generation of passivating species that occupy the active surface with the increase of polarization potential, leading to anodic current decrease and, subsequently, to occurrence of the negative R_p. In the

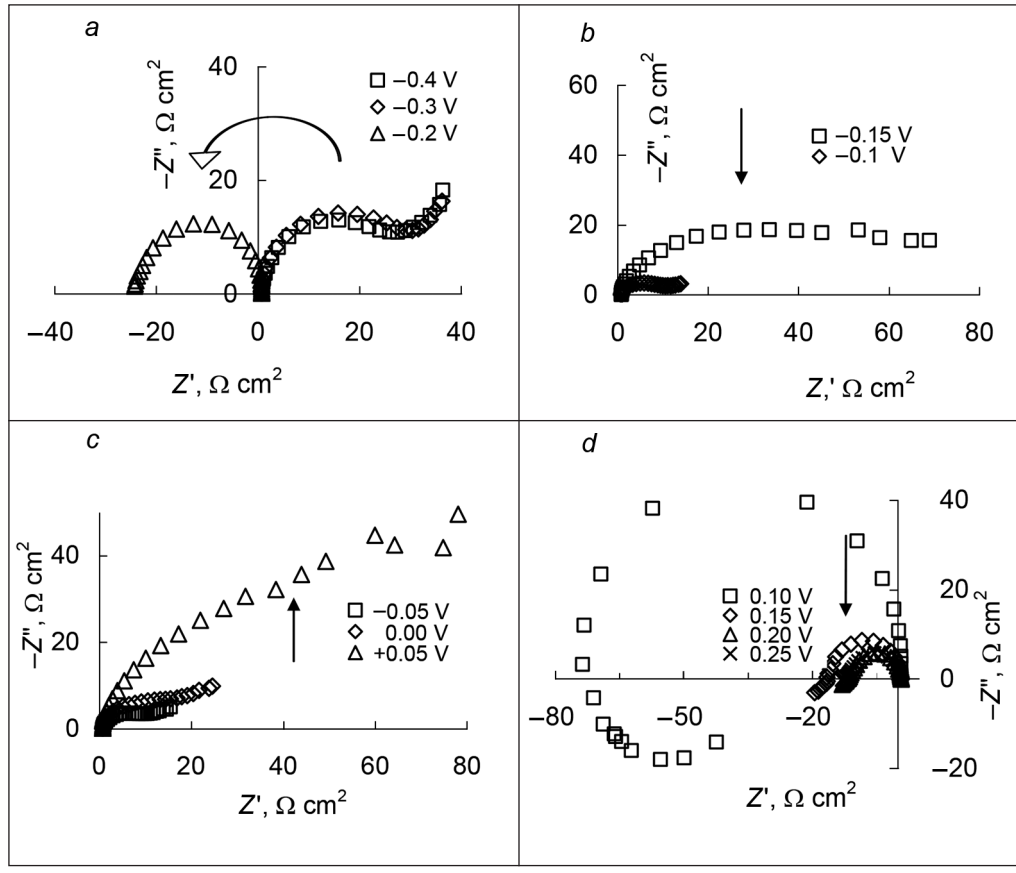

Fig. 3. Nyquist plots obtained for the Pt electrode in the 1 M NaOH + 0.05 M $NaBH_4$ solution at indicated potentials

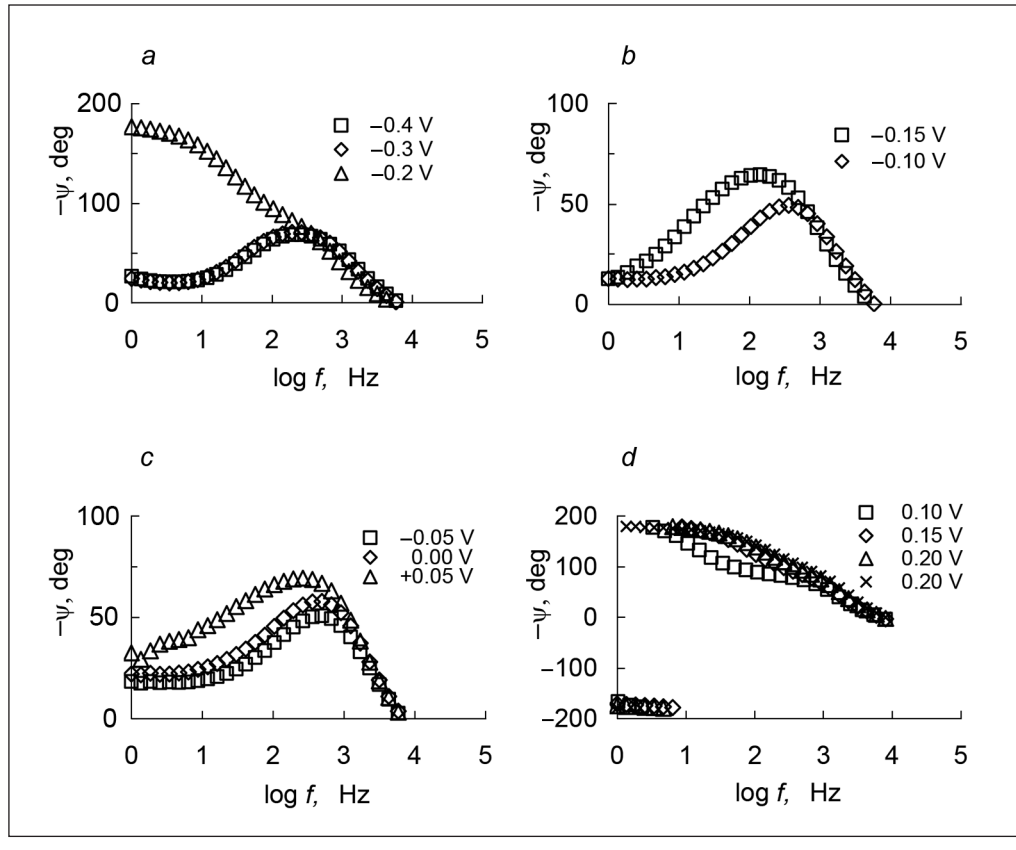

Fig. 4. Bode plots of the phase shift (ψ) obtained for the Pt electrode in the 1 M NaOH + 0.05 M $NaBH_4$ solution at indicated potentials

case of methanol electrooxidation Melnick and Palmore [47] indicated that the passivation of the Pt electrode appeared due to the reversible formation of oxide species often thought to be chemisorbed hydroxy radicals. The formation of a system with bifurcation and oscillatory conditions in the case of the formic acid electrooxidation were also analyzed for negative R_p [48].

Meanwhile, the observed phenomenon for borohydride oxidation implies that occurrence of negative R_p with the increase of E could be caused by the passivation of the Pt electrode due to the increasing generation of OH_{ad} on the surface in the presence of the accumulated borohydride intermediate species. The availability of free Pt sites, necessary for oxidation of borohydride species, decreases. The surface competition for reaction sites occurs. Following Density Functional Theory (DFT), a lot of species can be formed on the Pt electrode surface [12]. However, they are likely weakly adsorbed, quickly oxidize and rapidly transform into the products that easily desorb from the surface in that potential domain [11, 12, 26]. Therefore the decreasing anodic current leading to negative R_p could be appreciably related to increasing availability of oxygen-containing species on the Pt surface pointing to the change of borohydride oxidation mechanism. Another type of dissociative adsorption requiring only 1–3 free Pt atoms possibly occurs since an energetically favourable pathway with the minimum 9 free adjacent Pt atoms necessary for the dissociative adsorption of $BH_{4,ad}$ [11, 12, 26,] are most likely not available. Thus oxidation readily by OH_{ad} is expected [26].

At potentials between –0.15 and –0.1 V, the semi-circles in the Nyquist plots reverse to the first quadrant and the diameter of the arc decreases when E becomes more positive (Fig. 3b). One broad peak is observed in phase angle plots (Fig. 4b). It decreases and shifts toward higher frequency region suggesting that the rate of borohydride electrooxidation reaction grows up. It is supposed that in this E domain adsorbed OH_{ad} is involved in oxidation of borohydride species [26].

With further increase of the potentials from –0.05 to 0.05 V the diameter of the semicircle first starts to increase and then the impedance plot reverses again from the first quadrant to the second and enters the third quadrant at E = +0.1 V, roughly where we expect one complete monolayer of Pt oxide to be formed (Fig. 3c–d). The diameter of the loops decreases with the increase of the E indicating a decreasing R_p with the increase of potential (Fig. 3d). An abrupt jump between two unattached positive and negative values of phase angle appears as shown in Fig. 4d. The main reason is that the rate determining step of borohydride oxidation changes. Probably, it is related to change in the structure of the Pt surface oxide. Besides, EQCM results [26] revealed that the electrode mass decreased in the potential domain of wave a2 pointing to near complete consumption of all adsorbed species including OH_{ad}. The availability of OH_{ad} could become rate limiting. Therefore, adsorbed borohydride intermediate species ($BH_{3,ad}$ and BH_2 moiety, i. e. BH_2OH_{ad}, $BH_2OH^-_{ad}$, etc.) could start reacting with OH^- ions from solution by the Eley-Rideal-type mechanism [26, 11]. Furthermore, FTIR investigations showed that beyond E = +0.1 V BH_2 band intensity decreased, indicating the massive consumption of BH_2 species [11]. Although the formation of OH_{ad} and Pt oxides at high potentials inhibits borohydride oxidation, the oxygen-containing species, on the other hand, would facilitate the oxidation of BH_2 moiety and probably will be one of the reasons that would lead to reduced R_p (Fig. 3d).

To interpret EIS data of borohydride oxidation we made an attempt to analyse them by applying equivalent circuits (EC). In the case of oxidation of organic substances, mechanisms with adsorbed species are often invoked. EC used in this case have been overviewed by Lasia [49]. Generally, they contain such sub-circuits as the resistance, R, and the capacitance, C, in parallel, or R and the inductance, L, in series. Their description codes are (RC) and [RL], respectively. Here and below, elements in parallel are given in parenthesis and elements in series are enclosed in square brackets [50]. The above faradaic elements are usually shunted with the double layer impedance, Z_{dl}, and, finally, the ohmic resistance of the solution, R_Ω, is added. Such EC were used for studies of methanol [51, 52] and formic acid [48] oxidation on Pt electrodes. As for oxidation of borohydride, several rather complex equations were derived for impedance [28, 29] on Au without any EC specification. No EC specification was suggested for impedance in the case of borohydride oxidation on the Pt electrode in the presence of thiourea [19].

We failed to find a single EC that could be fitted over the entire range of the potentials under discussion. Different EC are normally used for differen potential regions in the case of oxidation of organic substances [48, 52]. Applied EC for EIS analysis and their description codes are shown in Fig. 5. We found that the impedance spectra obtained in the potential region of –0.4 V and –0.3 V can be described with frequency error ~3% by means of simplified EC denoted as (A) with the description code $R_\Omega(C_{dl}[RW])$, where W is the Warburg impedance. R_Ω was found to be independent on E and equal to 0.76 ± 0.01 Ω cm^2. Other parameters, determined at –0.4 V and –0.3 V, are rather close as well as the respective impedance spectra (Fig. 4a). An example of fitting results is shown in Fig. 6a.

We performed analysis with constant phase elements (CPE) Q_{dl} instead of double layer capacitance C_{dl}. The complex conductivity (Y) of CPE is equal to

$$Y = Y_0(j\omega)^n, \tag{11}$$

where $j = \sqrt{-1}$ [53]. At n = 1 the CPE transforms into capacitance with $Y_0 = C$. It was found that the factor n characterizing the element Q_{dl} is equal to 0.99–1. This fact gives ground to treat this CPE as C_{dl}.

However, for E = –0.3 V the EC denoted as (B) with the description code ($C_{dl}[RWC]$) in the presence of specifically

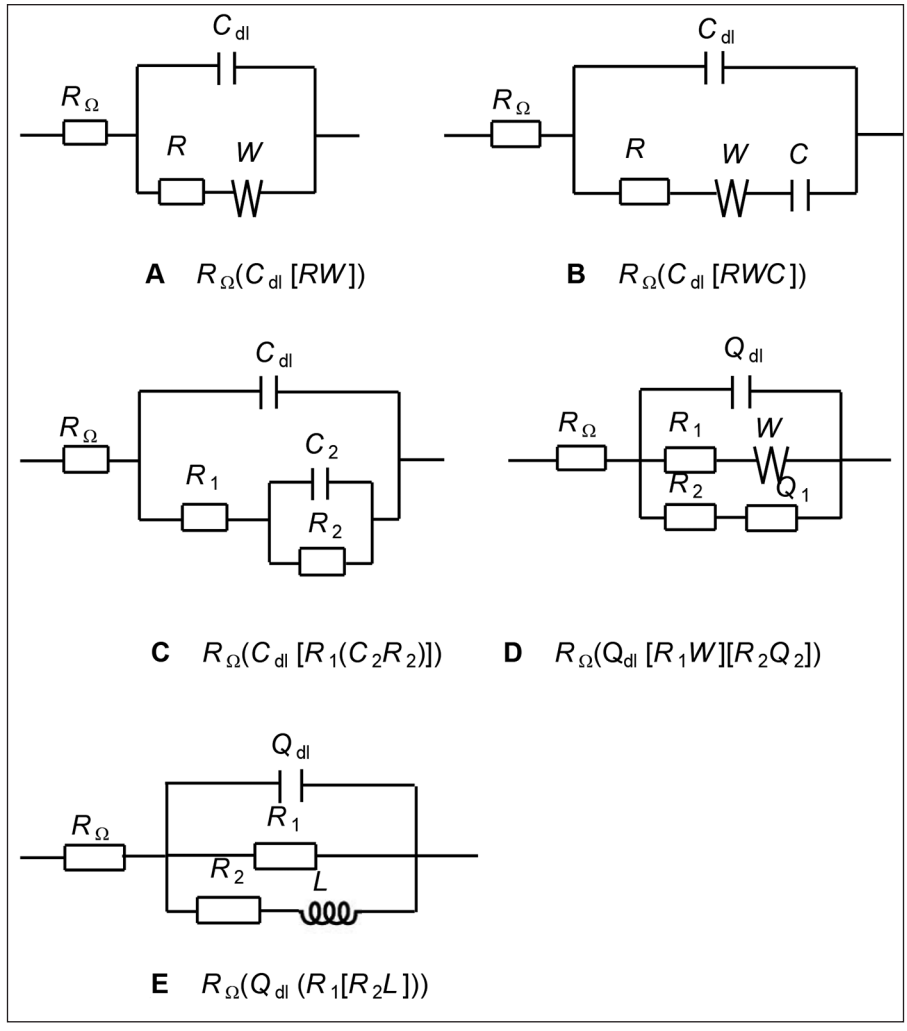

Fig. 5. Equivalent circuits used in this work

adsorbing species, or another denoted as (C) with the description code $R_\Omega(C_{dl}[R_1W(C_2R_2)])$ for electrochemical processes involving adsorption steps [49] fitted significantly better. However, negative R_1 and R_2 appeared in the latter case. Since the ultimate circuit gains too many adjustable parameters, its fit to the experimental data encounters a number of problems. Many ambiguous circuits are available, but they clearly point out to some adsorption features inherent to this potential region. An example of best fitting results for E = –0.3 V with the EC denoted as (B) is shown in Fig. 6b. It is necessary to point out that the change of BH_4^- oxidation mechanism occurs due of OH^- binding to the Pt surface [9]. It starts quite early in the alkaline medium as soon as desorption of H ceases [35, 36]. In contrast with other E regions, where the effect of forced convection is high, a very weak influence of rotating disk electrode rotation velocity was observed around the voltammetric dip at ca. –0.3 V and almost no effect of forced convection in it at ca. –0.2 V [9], where OH^- binding to Pt surface becomes more pronounced. A diminishing current density and other aforesaid factors offer a relative increase in the faradaic impedance making its elements undetectable. Therefore, the subcircuit denoted as (B) seems could be treated as some double-layer characteristic. Similar EC was proposed [54, 55] to describe adsorption layers whose formation is controlled by the rate of diffusion and electrosorption. A complicated mechanism of borohydride oxidation suggests a lot of species that could take part in adsorption processes [11, 12]. Therefore, it is hardly possible to propose an unambiguous treatment of the results obtained. Provided that borohydride dissociative adsorption is favoured all over the entire E region [12] and band intensity of p-polarized light for BH_4^- species starts growing above ca. –0.3 V, suggesting massive adsorption at the electrode surface [11], borohydride species can be supposed to be the primary substance that forms an adsorption layer. The presence of adsorbed borohydride species was also presumed [9, 26]. Another reliable alternative is the electrosorption of OH^- [9, 26] since generation of OH_{ad} is known to develop with E increased [34, 35].

In the voltammetric dip at ca. –0.2 V and around it slightly modified EC denoted as (C) with the description code $R_\Omega(C_{dl}[R_1(C_2R_2)])$ was applied. The oxidation current in the above mentioned potential domain has a negative

slope (Fig. 2), meaning that the impedance at zero frequency should be negative and is associated with the passivation of the Pt electrode due to increasing generation of OH_{ad}, as discussed above. We applied Q_{dl} and Q_2 instead of C_{dl} and C_2. Determined values n were close to 1. Furthermore, it appeared that the best fitting occurred with the negative R_2 provided no R_1 and W (Fig. 6c). Similar EC with negative R_2 and R_{ct} removed were applied for methanol oxidation [52].

At more positive potentials, where current density increases, the conductivity of the faradaic sub-circuit seems to grow. The general EC denoted as (D) with the description code $R_\Omega(Q_{dl}\ [R_1W][R_2Q_2])$ and its parameters are given in Fig. 6d. The double-layer impedance is presented by CPE Q_{dl}. As it is well known, at $n = -1, 0, 0.5$ or 1, Q transforms into L, R, W or C. Thus, the element Q_{dl} is of capacitive character as its parameter n is close or equal to 1. Two subcircuits,

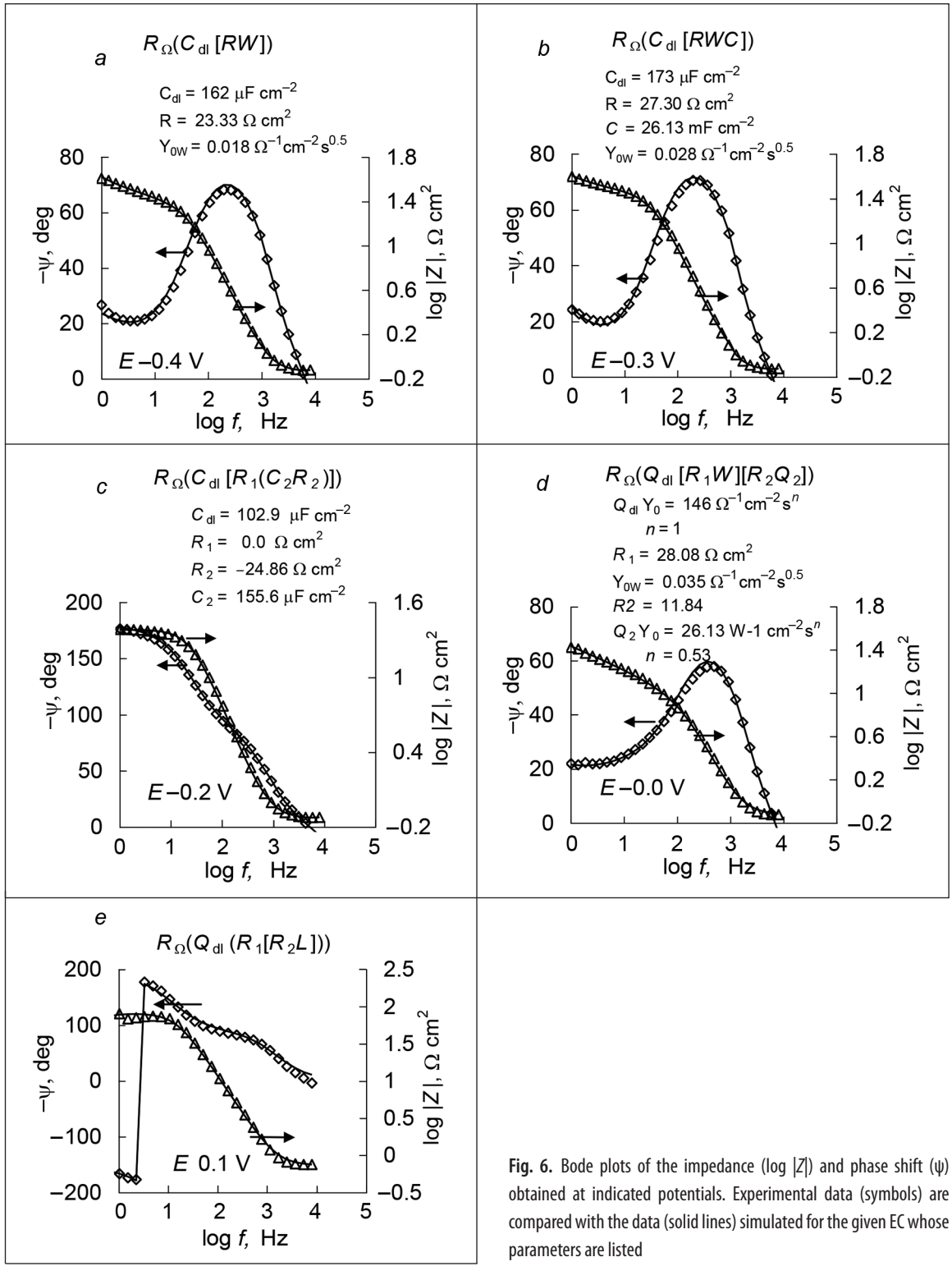

Fig. 6. Bode plots of the impedance (log |*Z*|) and phase shift (ψ) obtained at indicated potentials. Experimental data (symbols) are compared with the data (solid lines) simulated for the given EC whose parameters are listed

$[R_1W]$ and $[R_2Q_2]$, are rather similar since the average index n for Q_2 approaches 0.5. It is a problem to distinguish between these two subcircuits and to attribute the certain physical sense to them. One of them might be an analogue of the above subcircuit denoted as (B) for $E = -0.3$ V, another might be attributed to the diffusive flux of borohydride. At $-0.1 < E < 0.1$ V some parallel reactions seem to occur and mixed oxidation of BH_4^- and intermediate species is supposed [9].

With further increase of the potentials, starting from $E = 0.1$ V, where oxidation current has a negative slope again, the EC denoted as (E) with the description code $R_\Omega(Q_{dl}(R_1[R_2L]))$ fits. Negative R and L were applied.

It is appropriate to point out that in order to validate impedance data over entire E regions where positive or negative Z' was observed, the Kramers-Kronig (K-K) test [50] was used. Pseudo chi-squared fit values (χ^2), determined for positive impedance spectra at $-0.4 < E < 0.05$ V, lie between 10^{-4} and 10^{-5}. Hence, the K-K fit might be considered as marginal in this case. In contrast, high χ^2 values ranging up to $\sim 10^{-1}$ were obtained at $-0.2 < E < -0.15$ V and at $0.1 < E < 0.25$ V. This is indicative of rather low system stability over E regions where negative Z' is observed. Considering these results, a search for appropriate EC is worthwhile only in the former case, i. e. for positive impedance spectra. However, several EC [48, 52] were suggested for quasi steady-state or even for instable systems. Therefore we made an attempt to find the appropriate EC for negative Z' (Fig. 6c, e), but we do not go in for details if much useless derivation of EC fails when there is instability.

On the other hand, though experimental impedance spectrum is simple even for positive Z', the model deduced from the reaction mechanism may have too many adjustable parameters and data modeling is connected with the fact that the same data may be represented by different equivalent circuits [56]. The behaviours of these circuits in some cases are indistinguishable, that is when a proper choice of the parameters is performed they display the same impedance spectrum over all frequencies [49]. Thus, the obtained ECs in some potential regions are rather approximate, give only preliminary approach and particular examination is required. More detailed modeling of the impedance shapes in terms of the reaction steps will be pursued in order to gain more mechanistic details.

CONCLUSIONS

Borohydride oxidation on the polycrystalline Pt electrode was investigated in the aqueous alkaline medium by means of CV and EIS techniques. EIS data show a variety of spectral types of borohydride oxidation on Pt at E ranging from –0.4 V to 0.25 V and allow their direct correlation with the features of cyclic voltammogram. From experimental data it follows that both the low-frequency real component Z' and the steady-state voltammetric slope are of the same sign at the certain E. According to the sign of Z' in the Nyquist plots EIS spectra can be subdivided into two groups. In each group, Nyquist plots are quite similar in shape but differ in their quantitative characteristics depending on the E applied.

Negative R_p values determined in E regions at ca. –0.2 V and between +0.1 and +0.25 V are associated with the negative slope in the voltammogram and could be appreciably related to increasing availability of oxygen-containing species (OH_{ad} and / or Pt oxides) on the Pt surface in the presence of the accumulated borohydride species. The change in borohydride oxidation mechanism is supposed.

The observed impedance spectra for borohydride oxidation could be described by the means of EC presented in Fig. 5. No one single EC could be fitted over the entire potential domain. A search for appropriate EC is worthwhile only in the case of positive impedance spectra since the K-K test showed indications of rather low system stability over E regions where negative Z' is observed.

In the case of consumption of anodic wave a1, where positive Z' is observed, applied ECs clearly point to some adsorption features inherent to this potential region. Provided that borohydride species can be the primary substance that forms an adsorption layer, another reliable alternative is the electrosorption of OH^-.

The E region starting from –0.15 V, where positive Z' is observed again, can be described by adsorption of the above mentioned species for anodic wave a1 along with the diffusive flux that might be attributed to borohydride species. Some parallel reactions seem to occur.

Received 12 September 2013
Accepted 2 October 2013

References

1. C. Ponce de Leon, F. C. Walsh, D. Pletcher, D. J. Browning, J. B. Lakeman, *J. Power Sources*, **155**, 172 (2006).
2. J. Ma, N. A. Choudhury, Y. Sahai, *Renew. Sust. Energ. Rev.*, **14**, 183 (2010).
3. J.-H. Wee, *J. Power Sources*, **161**, 1 (2006).
4. J. P. Elder, A. Hickling, *Trans. Faraday Soc.*, **58**, 1852 (1962).
5. B. H. Liu, Z. P. Li, S. Suda, *Electrochim. Acta*, **49**, 3097 (2004).
6. E. Gyenge, M. Atwan, D. Northwood, *J. Electrochem. Soc*, **153**, A150 (2006).
7. L. C. Nagle, J. F. Rohan, *J. Electrochem. Soc.*, **153**, C773 (2006).
8. M. Chatenet, F. Micoud, I. Roche, E. Chainet, *Electrochim. Acta*, **51**, 5459 (2006).
9. D. A. Finkelstein, N. D. Mota, J. L. Cohen, H. D. Abruña, *J. Phys. Chem. C*, **113**, 19700 (2009).
10. M. Chatenet, F. H. B. Lima, E. A. Ticianelli, *J. Electrochem. Soc.*, **157**, B697 (2010).
11. B. M. Concha, M. Chatenet, E. A. Ticianelli, F. H. B. Lima, *J. Phys. Chem. C*, **115**, 12439 (2011).
12. G. Rostamikia, M. J. Janik, *Electrochim. Acta*, **55**, 1175 (2010).

13. M. C. S. Escaño, E. Gyenge, R. L. Arevalo, H. Kasai, *J. Phys. Chem. C*, **115**, 19883 (2011).
14. G. Rostamikia, M. J. Janik, *Electrochem. Soc.*, **156**, B86 (2009).
15. M. Chatenet, B. Molina Concha, G. Parrour, J. P. Diard, F. H. B. Lim, E. A. Ticianelli, in: U. Demirci, P. Miele (eds.), *Boron Hydrides, High Potential Hydrogen Storage Materials*, Ch. 5, Nova Science Publishers, New York (2010).
16. M. E. Indig, R. N. Snyder, *J. Electrochem. Soc.*, **109**, 1104 (1962).
17. M. V. Mirkin, H. Yang, A. J. Bard, *J. Electrochem. Soc.*, **139**, 2212 (1992).
18. M. H. Atwan, C. L. B. Macdonald, D. O. Northwood, E. L. Gyenge, *J. Power Sources*, **158**, 36 (2006).
19. E. Gyenge, *Electrochim. Acta*, **49**, 965 (2004.)
20. M. H. Atwan, D. O. Northwood, E. L. Gyenge, *Int. J. Hydrogen Energy*, **32**, 3116 (2007).
21. P. Krishnan, T.-H. Yang, S. G. Advani, A. K. Prasad, *J. Power Sources*, **182**, 106 (2008).
22. F. H. B. Lima, A. M. Pasqualeti, M. B. Molina Concha, M. Chatenet, E. A. Ticianelli, *Electrochim. Acta*, **84**, 202 (2012.)
23. B. Molina Concha, M. Chatenet, C. Coutanceau, F. Hahn, *Electrochem. Commun.*, **11**, 223 (2009).
24. B. Molina Concha, M. Chatenet, F. Mailard, E. A. Ticianelli, F. H. B. Lima, *J. Phys. Chem.*, **12**, 11509 (2010).
25. H. Dong, R. X. Feng, X. P. Ai, Y. L. Cao, H. X. Yang, C. S. Cha, *J. Phys. Chem. B*, **109**, 10896 (2005)
26. V. W. S. Lam, D. C. W. Kannangara, A. Alfantazi, E. L. Gyenge, *J. Phys. Chem. C*, **115**, 2727 (2011).
27. B. Molina Concha, M. Chatenet, *Electrochim. Acta*, **54**, 6119 (2009).
28. M. Chatenet, M. B. Molina-Concha, J.-P. Diard, *Electrochim. Acta*, **54**, 1687 (2009).
29. G. Parrour, M. Chatenet, J.-P. Diard, *Electrochim. Acta*, **55**, 9113 (2010).
30. B. V. Tilak, B. E. Conway, H. Angerstain-Kozlowska, *J. Electroanal. Chem.*, **48**, 1 (1973).
31. D. M. Dražić, A. V. Tripković, K. D. Popović, D. J. Lović, *J. Electroanal. Chem.*, **155**, 466 (1999).
32. N. M. Marković, T. J. Schmidt, B. N. Grgur, H. A. Gasteiger, P. N. Ross, Jr. R. J. Behm, *J. Phys. Chem. B*, **103**, 8568 (1999).
33. A. V. Tripković, K. D. J. Popović, D. J. Lović, *Electrochim. Acta*, **46**, 3163 (2001).
34. F. Kadirgan, B. Beden, F. C. Lamy, *J. Electroanal. Chem.*, **143**, 135 (1983).
35. N. M. Marković, H. A. Gasteiger, P. N. Ross, *J. Phys. Chem. B*, **100**, 6715 (1996).
36. N. M. Marković, S. T. Sarraf, H. A. Gasteiger, P. N. Ross, *J. Chem. Soc., Faraday Trans.*, **92**, 3719 (1996).
37. T. J. Schmidt, P. N. Ross, N. M. Marković, *J. Phys. Chem. B*, **105**, 12082 (2001).
38. C. Celic, F. G. Boyaci San, H. I. Sarac, *J. Power Sources*, **185**, 197 (2008).
39. K. J. J. Mayrhofer, G. K. H. Wiberg, M. Arenz, *J. Electrochem. Soc.*, **155**, P1 (2008).
40. R. Subbaraman, N. Danilovic, P. P. Lopes, D. Tripkovic, D. Strmcnik, V. R. Stamenkovic, N. M. Markovic, *J. Phys. Chem. C*, **116**, 22231 (2012).
41. I. Merino-Jimnez, C. Ponce de León, A. A. Shah, F. C. Walsh, *J. Power Sources*, **219**, 339 (2012).
42. D. A. Harrington, P. van den Driesshe, *Electrochim. Acta*, **56**, 8005 (2011).
43. C. N. Cao, *Electrochim. Acta*, **35**, 831 (1990).
44. C. N. Cao, *Electrochim. Acta*, **35**, 837 (1990).
45. M. Keddam, O. R. Mattos, H. Takenouti, *Electrochim. Acta*, **31**, 1147 (1986).
46. R. D. Armstrong, *J. Electroanal. Chem.*, **34**, 387 (1972).
47. R. E. Melnick, G. T. R. Palmore, *J. Phys. Chem. B*, **105**, 9449 (2001).
48. F. Seland, R. Tunold, D. A. Harrington, *Electrochim. Acta*, **53**, 6851 (2008).
49. A. Lasia, in: B. E. Konway, J. Bocris, R. E. White (eds.), *Modern Aspects of Electrochemistry*, Vol. 32, P. 29–36, Kluwer Academic / Plenum, New York (1999).
50. B. A. Boukamp, *J. Electrochem. Soc.*, **142**, 1885 (1995).
51. I.-M. Hsing, X. Wang, Y-J. Leng, *J. Electrochem. Soc.*, **149**, A615 (2002).
52. F. Seland, R. Tunold, D. Harrington, *Electrochim. Acta*, **51**, 3827 (2006).
53. J. R. Macdonald, *Impedance Spectroscopy*, John Wiley & Sons, New York (1987).
54. A. Frumkin, V. I. Melik-Gaikasian, *Dokl. Akad. Nauk SSSR*, **77**, 855 (1951).
55. V. I. Melik-Gaikasian, *Zh. Fiz. Khim.*, **26**, 560 (1952).
56. P. Zoltowski, *J. Electroanal. Chem.*, **375**, 45 (1994).

Dijana Šimkūnaitė, Loreta Tamašauskaitė-Tamašiūnaitė, Svetlana Lichušina

BOROHIDRIDO ELEKTROOKSIDACIJA ANT POLIKRISTALINĖS PLATINOS ELEKTRODO

S a n t r a u k a

Buvo tirta borohidrido oksidacija ant Pt elektrodo šarminiuose tirpaluose, turinčiuose 0,05 M $NaBH_4$ ir 1 M NaOH, panaudojant EIS ir ciklinės voltametrijos metodus. Srovės tankio pokyčiai nagrinėti lyginant juos su EIS matavimų duomenimis. Manoma, kad mažėjančios anodinės srovės sritys, sąlygojančios neigiamą R_p atsiradimą, yra susijusios su deguonį turinčių darinių (OH ir Pt oksidų) buvimu ant Pt elektrodo paviršiaus, kartu kaupiantis ir įvairiems borohidrido dariniams. Aptarti galimi borohidrido oksidacijos procesai bei elektrinės grandinės atsižvelgiant į naudotą potencialo sritį. Skirtingose potencialų srityse taikomos skirtingos elektrinės grandinės.